

Highly Sensitive Amperometric Sensor for the Determination of Glucose at Histidine Stabilized Copper Nanospheres Decorated Multi-Walled Carbon Nanotubes

Shen-Ming Chen^{1,*}, Rajkumar Devasenathipathy^{1,2}, Sea-Fue Wang^{2,*}, Karuppasamy Kohilarani²

¹ Electroanalysis and Bioelectrochemistry Lab, Department of Chemical Engineering and Biotechnology, National Taipei University of Technology, No. 1, Section 3, Chung-Hsiao East Road, Taipei 106, Taiwan, ROC.

² Department of Materials and Mineral Resources Engineering, No. 1, Sec. 3, Chung-Hsiao East Rd., National Taipei University of Technology, Taipei, Taiwan

*E-mail: smchen78@ms15.hinet.net, sfwang@ntut.edu.tw

Received: 13 March 2016 / Accepted: 11 May 2016 / Published: 4 June 2016

Uniform sized copper nanospheres (CuNSs) were deposited at functionalised multiwalled carbon nanotubes (f-MWCNTs) modified glassy carbon electrode (GCE) through a simple electrochemical method. Here, biomolecule (histidine) is used as stabilizing agent for the synthesis of copper nanospheres. The prepared nanocomposite was characterized by scanning electron microscopy (SEM), Energy-dispersive X-ray spectroscopy (EDX) and X-ray diffraction spectroscopy (XRD). The f-MWCNTs/CuNSs modified GCE exhibited a good electrocatalytic activity towards the determination of glucose. Our sensor showed a wide linear range from 10 μM to 6910 μM with LOD of 1.53 μM towards glucose. The sensitivity of our sensor is 1.39 $\mu\text{A}\mu\text{M}^{-1}\text{cm}^{-2}$. In addition, the sensor attained an appreciable stability, repeatability and reproducibility. Practicality of our sensor was demonstrated in the human serum samples. Simplicity, biocompatibility, cost effectiveness, and highly stability of electrode surface are the main advantages our fabricated modified electrode.

Keywords: Copper nanospheres, histidine, MWCNTs, glucose, practicality.

1. INTRODUCTION

The development of conventional electrochemical biosensors for the determination of glucose especially in food industry and medical field have been considerably important for the past few years [1, 2]. Glucose oxidase and glucose dehydrogenase are the most extensively used enzymes in the electrochemical glucose biosensors[3, 4]. Nonetheless, some of the main obstacles such as enzyme leaching, complex immobilization, and instability at elevated temperature and pH are there for the

immobilization of enzyme on the electrode surface or electrode modified surface[5]. To minimize this difficulties, non-enzymatic or enzyme free glucose sensors have been used as alternative sensors [6, 7]. Numerous modified electrode materials such as metal nanoparticles, metal oxides and alloy compounds have been reported for the non-enzymatic detection of glucose in alkaline medium[8]. Especially, the higher abundance, and low cost of metals and metal oxides (Cu, Cu₂O, Ni, NiO, Co₃O₄, etc.) are highly desirable in the electroanalytical community[9-12].

Copper is one of the potentially available alternative to gold, platinum and palladium because of its higher abundance, low cost, and biocompatibility [13]. Moreover, copper nanoparticles provide larger surface-to-volume ratio compared to its micro and macro particles which have been widely used in many applications such as catalysis, medicine, sensors and infrared sensing materials[14]. Thus, several researchers have focused on the preparation of copper nanoparticles for the determination of glucose. However, the preparation of copper nanoparticles has been challenging because of its easy oxidation in air, aggregation and instability[15]. To minimize this key issues, ligands or capping agents have been used in recent years[16]. Notably, some of the amino (-NH₂) and hydroxyl (-OH) groups enriched biomolecules such as choline chloride-urea and citric acid were reported as stabilizing agents for the controlled synthesis of copper nanoparticles through electrochemical method[17, 18].

Since stabilizing agents play a vital role in the controlled synthesis of copper nanoparticles, we have utilized histidine as stabilizing agent for the electrochemical synthesis of Copper nanospheres which contains imidazole ring along with amino and carboxylic groups[19, 20]. Recently, we have reported an electrochemical sensor for the determination of hydrogen peroxide based on histidine stabilized copper nanoparticles decorated on graphene nanosheets [21]. In this work, MWCNTs are used as supporting mat for anchoring the copper nanospheres because of its rapid electrode kinetics, large surface area, high conductivity, outstanding electrocatalytic ability, promoting electron transfer reactions at a lower over potential and less fouling effect [15, 22]. Moreover, several MWCNTs based copper nanoparticles modified electrodes have also been fabricated in other applications of biosensor, photo generator and fuel cell in recent years [23-25].

The main aim of this work is to fabricate uniform sized electroactive copper nanospheres using histidine (stabilizing agent) at MWCNTs modified electrode for the effective determination of glucose. The f-MWCNTs/CuNSs modified GCE showed a good electrocatalytic activity towards the determination of glucose in alkaline media compared to other modified GCEs. The fabricated non enzymatic glucose sensor exhibited a low limit of detection (LOD), wider linear response and fast response for the determination of glucose.

2. EXPERIMENTAL

2.1 Reagents and apparatus

MWCNTs, copper (II) nitrate dihydrate (Cu(NO₃)₂ · 2H₂O), L-Histidine and D+ glucose were purchased from Sigma Aldrich. All other chemicals used were of ACS-certified reagent grade and used without further purification. The supporting electrolyte used for all the electrochemical studies was 0.1

M NaOH. Prior to each experiment, all the solutions were deoxygenated with pre-purified N₂ gas for 15 min unless otherwise specified. Double distilled water with conductivity of $\geq 18 \text{ M}\Omega \text{ cm}^{-1}$ was used for all the experiments. Human blood serum samples were collected from valley biomedical, Taiwan product & services, Inc. This study was reviewed and approved by the ethics committee of Chang-Gung memorial hospital through the contract no. IRB101-5042A3

2.2 Apparatus

Electrochemical measurements were carried out using CHI 611A work station in a conventional three electrode cell with modified GCE (area 0.071 cm^2), saturated Ag|AgCl (saturated KCl) and Pt wire as a working, reference and counter electrodes, respectively. Amperometric measurements were performed with analytical rotator AFMSRX (PINE instruments, USA) and rotating disc glassy carbon electrode (RDE, area 0.21 cm^2). Scanning electron microscope (SEM) and Energy-dispersive X-ray (EDX) spectra were carried out using Hitachi S-3000 H scanning electron microscope and HORIBA EMAX X-ACT, respectively. X-ray diffraction (XRD) studies were carried out in XPERT-PRO diffractometer using Cu K α radiation ($k=1.54 \text{ \AA}$).

2.1 Preparation and fabrication of f-MWCNTs/ CuNSs/GCE.

First, MWCNTs were functionalised using the previously reported procedure. Typically, 0.1 g of MWCNTs were added in to a beaker containing 12 ml 0.4 M HCl (aqueous solutions) and it was sonicated for 4 hours. Then, 12 ml concentrated H₂SO₄–HNO₃ (3 :1) solution was added in to the mixture and refluxed for 4 hours. Finally, the obtained functionalised MWCNTs (f–MWCNTs) were washed several times with deionised water until the pH of filtrate became 7. The f–MWCNTs precipitate was dried in air oven at 70^o C for 12 hours.

The fabrication of f–MWCNTs/His–CuNSs/GCE involves a single step process. 10 μl of aqueous f–MWCNTs (1mg/ml) was drop cast on a pre-cleaned GCE and dried at ambient conditions. f–MWCNTs/GCE was dipped into an electrochemical cell containing 10 mM Cu(II) and 20 mM histidine solutions (1:2). Then, electrochemical deposition of copper nanospheres at f–MWCNTs/GCE was carried out at the potential of -0.6 V (Ag|AgCl) for 600s. As control, other modified electrodes such as only CuNSs/GCE and Copper/GCE in the absence of stabilizing agent histidine (we abbreviated CuNPs/GCE for the sake of simplicity) were also fabricated using the similar procedure.

3. RESULT AND DISCUSSION

3.1. Characterization of f-MWCNTs/CuNSs/GCE composite

Scanning electron microscopy (SEM) was used to characterize the morphology of prepared nanocomposites and their results are given in Fig.1A&B. The SEM image of histidine stabilized copper shows uniform deposition of nanospheres at the surface of electrode (Fig.1A). The average size

of nanoparticles was found to be 70 ± 20 nm. This can be due the strong coordinated covalent interaction between the histidine and Cu(II) ions. Moreover, the electrostatic interaction between the positively charged Cu^{2+} cations and negatively charged histidine anion offers a higher stability for the formation of copper(II)-bis(L-histidinato) $[\text{Cu}[\text{His}]_2]$ complex[26]. For control, only copper was deposited in the absence of histidine (stabilizing agent). The deposited copper showed highly aggregated nanoparticles and size of the nanoparticles are larger than that of histidine stabilized copper nanoparticles (Figure not shown). The SEM image of f-MWCNTs/CuNSs is presented in Fig.1B. It shows that f-MWCNTs are decorated by a number of copper nanospheres. Moreover, the figure apparently indicates that the prepared nanospheres are presented at the surface of CNTs. The uniform shape of CuNSs confirms the controlled synthesis of copper nanospheres. The corresponding Energy-dispersive X-ray (EDX) signals of f-MWCNTs/CuNSs film (Fig. 1C) display the presence of elements namely, C, N, O and Cu with weight percentage of 42.25, 4.09, 5.46 and 48.20%, respectively. The presence of considerable amount of nitrogen and oxygen clearly indicates the role of histidine (stabilizing agent) for the uniform deposition of copper nanospheres at the surface of f-MWCNTs.

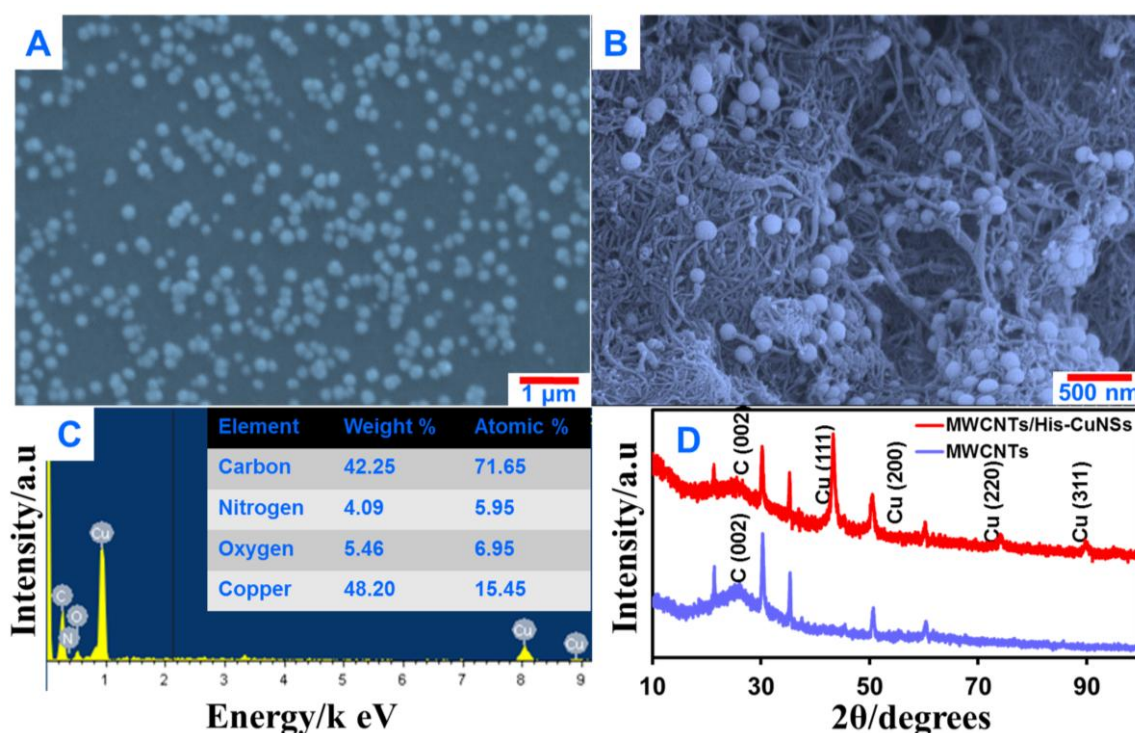


Figure 1. SEM images of CuNSs (A) and f-MWCNTs/CuNSs (B), EDX spectra of f-MWCNTs/CuNSs (C) and XRD pattern of f-MWCNTs/CuNSs (D).

X-ray diffraction pattern of f-MWCNTs/CuNSs (Fig.1D) shows four well-defined diffraction peaks at 43.33° , 50.63° , 74.75° and 89.9° corresponding to the planes of Histidine-CuNSs [(111), (200) (220) and (311)] which is in concordance with the previously reported metallic copper nanoparticles (JCPDS) [27]. One more diffraction peak appeared at 2θ of 26.3° can be the graphitic

network of carbon nanotubes which is confirmed by XRD pattern of only MWCNTs [28]. The XRD peaks of ITO are indicated by the symbol (*).

3.2 Electrooxidation of glucose at various modified electrodes

Cyclic voltammetry was used to study the electrooxidation of glucose at various modified GCEs such as CuNPs (in the absence of histidine), CuNSs and f-MWCNTs/CuNSs/GCE in 0.1 M NaOH containing 5 mM glucose and their corresponding results are given in Fig.2A. Only copper nanoparticles (without using stabilizing agent) modified GCE displayed a sigmoidal type of curve at the potential of 0.583V (Ag|AgCl), which indicates the slow electron transfer kinetic process of glucose at CuNPs/GCE. While, CuNSs showed a well-defined peak and lower over potential (0.465 V (Ag|AgCl) compared to only CuNPs/GCE, reveals the good electrocatalytic activity of CuNSs towards glucose oxidation which may be due to the controlled deposition of copper nanospheres at the surface of electrode. The f-MWCNTs/CuNSs/GCE showed an enhanced oxidation peak at 0.441V (Ag|AgCl) which is nearly two fold increased peak current compared to peak current obtained at CuNSs/GCE. It can be attributed to the good electrical conductivity and catalytic properties of f-MWCNTs which induces the electron transfer reaction between glucose and electrode. From the results of observation, it is clearly understood that copper nanospheres exhibit good electro catalytic ability for the oxidation of glucose and f-MWCNTs exhibits good conductance for the electrooxidation of glucose.

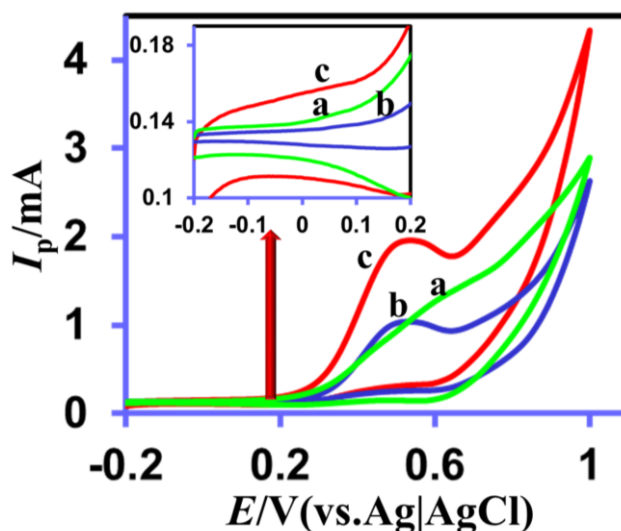


Figure 2. (A) CVs obtained at CuNPs (A), CuNSs (B) and f-MWCNTs/CuNSs films modified GCEs in 0.1 M NaOH containing 5 mM glucose at the scan rate of 50 mV s⁻¹.

In addition, the role of stabilizing agent for the uniform deposition of copper nanoparticles and conductance of f-MWCNTs were confirmed by CV. Inset to Fig.1 shows capacitance current of absence (a) and presence of histidine stabilized copper nanospheres (b) and f-MWCNTs/CuNSs (c). As can be seen in figure, the capacitive current of histidine stabilized copper nanospheres is lower

compared to copper nanoparticles (without histidine). It must be due to the thick coating of organic ligand, histidine (stabilizing agent) on the surface of CuNSs. The f-MWCNTs/CuNSs/GCE shows higher capacitance relative to only copper and CuNSs, indicating that f-MWCNTs induce the rapid electron transferring ability of modified electrode.

3.3 Effect of scan rate on oxidation of glucose

CV technique was used to study the effect scan rate at f-MWCNTs/CuNSs/GCE in 0.1M NaOH containing 5 mM glucose. Fig. 3A shows CVs of f-MWCNTs/CuNSs modified GCE at different scan rates from 0.1 to 0.8 Vs⁻¹. As can be seen in figure, the peak current of 5 mM glucose increased as the scan rate of modified electrode increases. Moreover, the calibration plot between anodic peak current of modified electrode vs scan rate is obtained linear dependence (Fig. 3B). The result indicates that the electrooxidation of glucose at modified electrode follows surface-confined electrochemical process[29].

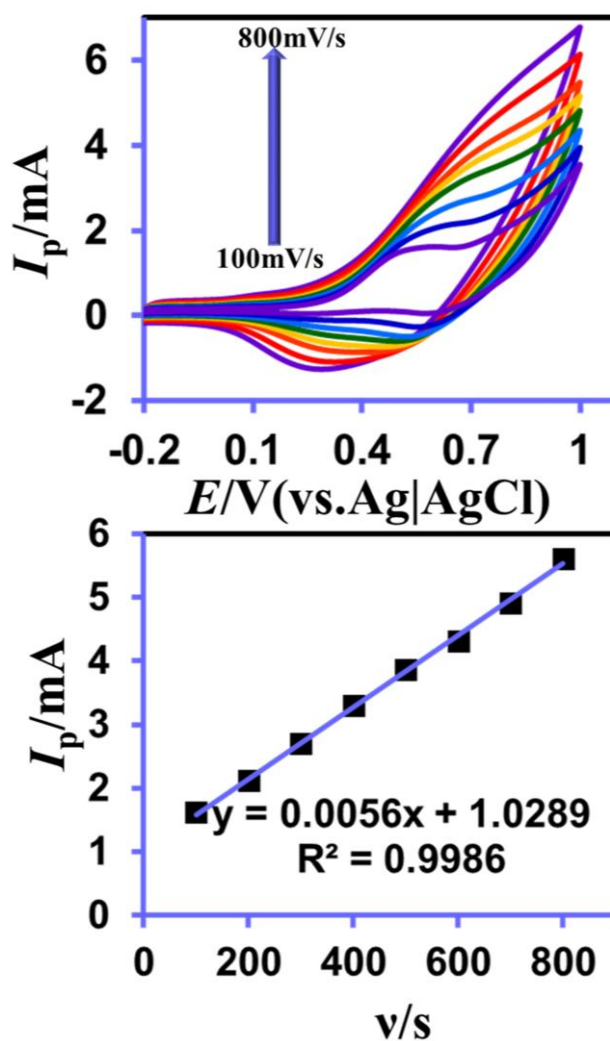


Figure 3.(A) CVs obtained at f-MWCNT/CuNSs/GCE for various scan rates (from 20 mVs⁻¹ to 160 mVs⁻¹) in 0.1 M NaOH containing 5 mM glucose. (B) Calibration plot between I_p vs v .

3.4. Amperometric determination of glucose

The sensitive detection of glucose at f-MWCNTs/CuNSs/GCE was carried out by using amperometry. Fig. 4A displays the amperograms of f-MWCNTs/CuNSs modified GCE for each addition of different concentrations of glucose (10, 100 and 1000 μM) into the 0.1 M NaOH solution. The potential and rotation speed were set at 0.4 V and 1500 rpm. An increasing well-defined and stable amperometric response was observed for each addition of glucose with increasing concentration. From the calculated response time of our modified electrode (3s), it is evident that the f-MWCNTs/CuNSs/GCE offers a fast response towards oxidation of glucose. In addition, a linear dependency was observed from the calibrated plot between amperometric response (I_p) and concentration of glucose (Fig. 4B). The analytical parameters such as linear range, LOD and sensitivity of fabricated sensor was calculated from the linear regression equation ($I_p/\mu\text{A} = 0.0056 [\text{glucose}]/\mu\text{M} \mu\text{M}^{-1} + 1.0289$; $R^2=0.998$) as 10 μM to 6.910 μM , LOD of 1.53 μM ($S/N=3$) and 1.39 $\mu\text{A}/\mu\text{M cm}^2$ towards glucose respectively. The corresponding reaction mechanism for electrooxidation of glucose at f-MWCNT/CuNSs/ GCE is given below [30],

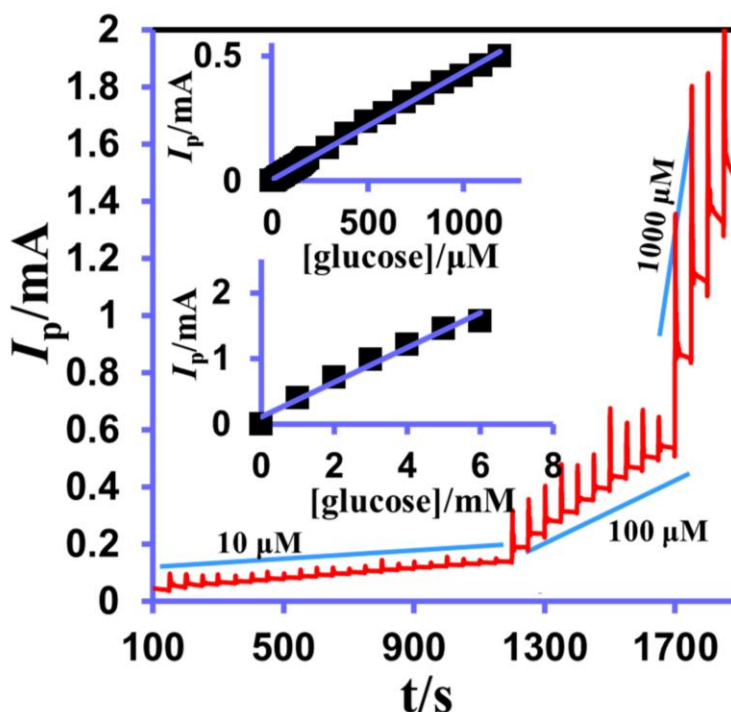
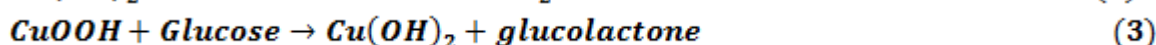
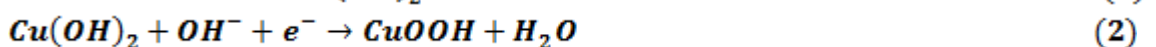


Figure 4. (A) Amperograms of f-MWCNT/CuNSs film modified rotating disc GCE upon addition of 10 μM , 100 μM and 1000 μM glucose into 0.1M NaOH at the rotation speed of 1500 rpm at $E_{\text{app}} = +0.40$ V. (B) Plot of [glucose] vs. I_p .

The obtained electroanalytical parameters were compared with the previously reported non-enzymatic glucose modified electrodes (**Table.1**). The results of linear range, LOD and sensitivity confirmed that our f-MWCNT/CuNSs/GCE shows comparable performance with previously reported non-enzymatic glucose sensors for the determination of glucose.

Table 1. Comparison of electroanalytical parameters obtained at f-MWCNTs/CuNSs/GCE with other previously reported modified electrodes.

Modified electrode (GCE)	Linear range (mM)	Sensitivity ($\mu\text{A}\mu\text{M}^{-1}\text{cm}^{-2}$)	LOD (μM)	Ref.
Cu ₂ O NCs/graphene nanosheets	0.3–3.3	0.285	3.34	[31]
Co ₃ O ₄ ultra nanosheet-Ni(OH) ₂	0.005–40	1.089	1.08	[32]
Nanoporous CoNWs	0.005–5.7	0.300	5	[6]
Cu nanowires	0.005–6.0	1.100	0.6	[33]
ultrafine Co ₃ O ₄ nanocrystals	0.01–0.8	2.597	1.0	[34]
Porous Cobalt oxide	0.49–1.92	0.426	0.16	[35]
Cubic Cu ₂ O	0.0005–6	–	0.3	[36]
Ni-Co nanosheets/RGO	0.01–2.65	1.773	3.79	[37]
Cu/Cu ₂ O nanocluster	10–690	0.022	5	[38]
Cu-Co Nano sheets	0.015–6.95	1.91	10	[39]
Porous Co nanobeads/RGO	0.15–6.25	0.039	47.5	[40]
Carbon quantum dots/Cu ₂ O	0.020–4300	0.298	8.4	[41]
f-MWCNTs/CuNSs	0.01–6.910	1.39	1.53	This work

3.5 Selectivity,

For the selectivity of our glucose sensor, common interfering biological compounds such as dopamine, ascorbic acid and uric acid were chosen. There is no obvious response upon addition of 0.1 mM of dopamine (DA), uric acid (UA) and ascorbic acid (AA) in the amperometric i-t response of f-MWCNT/CuNSs/GCE **along with** 1 mM glucose. This shows the selective detection of glucose by our modified electrode in the presence of other interfering biomolecules.

3.6 Stability, repeatability and reproducibility

For evaluating the storage stability of our fabricated **f-MWCNT/CuNSs/GCE**, the electrocatalytic response of our modified electrode towards electro-oxidation of glucose was monitored every day. 95.52% of the initial I_{pa} was retained over a month of its continuous use. This indicates that the fabricated modified electrode has good storage stability. In addition, Repeatability and reproducibility of our sensor were also evaluated in 0.1 M NaOH containing 500 μM glucose. The **f-MWCNT/CuNSs/GCE** attained an appreciable repeatability with relative standard deviation (R.S.D) of 2.86% for 5 repetitive measurements which were performed by a single **f-MWCNT/CuNSs** modified **GCE**. Moreover, significant reproducibility of 3.2% was calculated by our modified

electrode for 5 independent measurements which was carried out in 5 different f-MWCNT/CuNSs modified GCEs.

3.7. Practicality

Human blood serum samples were chosen for evaluation of practical applicability of developed sensor. Thus, some of the human serum samples were received from normal and diabetic patients. Moreover, concentration of glucose present in the blood serum samples was already predetermined by commercial Tecan Sunrise plate reader. Amperometric *i-t* method was used in our work for the determination of glucose present in the obtained human serum samples (experimental condition is same as section 3.4) and their results are in good agreement with commercial sensor (Table.2). This confirms the practical feasibility of our sensor for the detection of glucose in clinical samples.

Table 2. Determination of glucose in normal and diabetic patients blood serum samples.

Serum sample	Glucose detected by commercial detector	Glucose detected by our sensor (mM)	Recovery (%)	RSD
1	5.05	5.19	102.7	3.6
2	4.12	4.18	101.4	2.9
3	7.12	7.04	98.8	4.2

4. CONCLUSIONS

In summary, f-MWCNTs/ CuNSs nanocomposite was successfully prepared via simple electrochemical potentiostatic method. Scanning electron microscopy was utilized to confirm the morphology of f-MWCNTs/ CuNSs nanocomposite. elemental composition of nanocomposite of nanocomposite was confirmed by EDX spectroscopy. While, crystal structure of the nanocomposite was confirmed by XRD spectroscopic study. f-MWCNTs/ CuNSs/GCE showed a satisfactory electroanalytical performance in terms of wide linear range from 10 μM to 6910 μM with LOD of 1.53 μM . The sensitivity of our modified electrode attained 1.39 $\mu\text{A}\mu\text{M}^{-1}\text{cm}^{-2}$. These electroanalytical parameters of the fabricated modified electrode were quite comparable to the previously reported glucose sensor. In addition, the practicality of our sensor was evident from the accurate determination of glucose in human serum samples. The sensor showed an appreciable stability, repeatability, and reproducibility.

ACKNOWLEDGEMENTS

Dr. Rajkumar Devasenathipathy gratefully acknowledges the National Taipei University of Technology, Taiwan for the postdoctoral fellowship.

References

1. E.C. Alocilja, S.M. Radke, Market analysis of biosensors for food safety, *Biosensors and Bioelectronics* 18(5) (2003) 841-846.
2. R. Devasenathipathy, V. Mani, S.-M. Chen, S.-T. Huang, T.-T. Huang, C.-M. Lin, K.-Y. Hwa, T.-Y. Chen, B.-J. Chen, *Enzyme and microbial technology* 78 (2015) 40-45.
3. Ö. Sağlam, B. Kızılkaya, H. Uysal, Y. Dilgin, *Talanta* 147 (2016) 315-321.
4. F.S. Saleh, L. Mao, T. Ohsaka, *Sensors and Actuators B: Chemical* 152(1) (2011) 130-135.
5. K.E. Toghiani, R.G. Compton, *Int J Electrochem Sci* 5(9) (2010) 1246-1301.
6. L. Kang, D. He, L. Bie, P. Jiang, *Sensors and Actuators B: Chemical* 220 (2015) 888-894.
7. S. Park, H. Boo, T.D. Chung, *Analytica Chimica Acta* 556(1) (2006) 46-57.
8. V. Mani, R. Devasenathipathy, S.-M. Chen, J.-A. Gu, S.-T. Huang, *Renewable Energy* 74 (2015) 867-874.
9. A.A. Ensafi, M.M. Abarghoui, B. Rezaei, *Electrochimica Acta* 123 (2014) 219-226.
10. Y. Zhao, X. Bo, L. Guo, *Electrochimica Acta* 176 (2015) 1272-1279.
11. R.A. Soomro, A. Nafady, Z.H. Ibupoto, S.T.H. Sherazi, M. Willander, M.I. Abro, *Materials Science in Semiconductor Processing* 34 (2015) 373-381.
12. K.-C. Lin, Y.-C. Lin, S.-M. Chen, *Electrochimica Acta* 96 (2013) 164-172.
13. P. Karthik, S.P. Singh, *RSC Advances* 5(79) (2015) 63985-64030.
14. A. Kumar, A. Saxena, A. De, R. Shankar, S. Mozumdar, *Rsc Advances* 3(15) (2013) 5015-5021.
15. S.M. Lin, S. Geng, N. Li, N.B. Li, H.Q. Luo, *Talanta* (2016).
16. L.K. Sannegowda, K.V. Reddy, K. Shivaprasad, *RSC Advances* 4(22) (2014) 11367-11374.
17. Q. Zhang, Y. Hua, *Physical Chemistry Chemical Physics* 16(48) (2014) 27088-27095.
18. M.V. Mandke, H.M. Pathan, *Journal of Electroanalytical Chemistry* 686 (2012) 19-24.
19. T. Venelinov, S. Arpadjan, I. Karadjova, J. Beattie, *ACTA PHARMACEUTICA-ZAGREB-* 56(1) (2006) 105.
20. T. Szabó-Plánka, A. Rockenbauer, L. Korecz, D. Nagy, *Polyhedron* 19(9) (2000) 1123-1131.
21. R. Devasenathipathy, K. Kohilarani, S.-M. Chen, S.-F. Wang, S.-C. Wang, C.-K. Chen, *Electrochimica Acta* (2016).
22. M. Roushani, K. Bakyas, B.Z. Dizajdizi, *Materials Science and Engineering: C* 64 (2016) 54-60.
23. M. Scarselli, C. Scilletta, F. Tombolini, P. Castrucci, M. Diociaiuti, S. Casciardi, E. Gatto, M. Venanzi, M. De Crescenzi, *The Journal of Physical Chemistry C* 113(14) (2009) 5860-5864.
24. S. Chawla, R. Rawal, C. Pundir, *Journal of biotechnology* 156(1) (2011) 39-45.
25. H. Rostami, A.A. Rostami, A. Omrani, *Electrochimica Acta* 194 (2016) 431-440.
26. P. Deschamps, P. Kulkarni, M. Gautam-Basak, B. Sarkar, *Coordination chemistry reviews* 249(9) (2005) 895-909.
27. B.K. Park, S. Jeong, D. Kim, J. Moon, S. Lim, J.S. Kim, *Journal of colloid and interface science* 311(2) (2007) 417-424.
28. H.-X. Wu, W.-M. Cao, Y. Li, G. Liu, Y. Wen, H.-F. Yang, S.-P. Yang, *Electrochimica Acta* 55(11) (2010) 3734-3740.
29. R. Devasenathipathy, C. Karuppiyah, S.-M. Chen, S. Palanisamy, B.-S. Lou, M.A. Ali, F.M. Al-Hemaid, *RSC Advances* 5(34) (2015) 26762-26768.
30. T. Yang, J. Xu, L. Lu, X. Zhu, Y. Gao, H. Xing, Y. Yu, W. Ding, Z. Liu, *Journal of Electroanalytical Chemistry* 761 (2016) 118-124.
31. M. Liu, R. Liu, W. Chen, *Biosensors and Bioelectronics* 45 (2013) 206-212.
32. M. Mahmoudian, W. Basirun, P.M. Woi, M. Sookhakian, R. Yousefi, H. Ghadimi, Y. Alias, *Materials Science and Engineering: C* 59 (2016) 500-508.
33. Z. Fan, B. Liu, X. Liu, Z. Li, H. Wang, S. Yang, J. Wang, *Electrochimica Acta* 109 (2013) 602-608.
34. M. Li, C. Han, Y. Zhang, X. Bo, L. Guo, *Analytica chimica acta* 861 (2015) 25-35.
35. Y. Song, J. He, H. Wu, X. Li, J. Yu, Y. Zhang, L. Wang, *Electrochimica Acta* 182 (2015) 165-172.

36. H. Li, J. Li, D. Chen, Y. Qiu, W. Wang, *Sensors and Actuators B: Chemical* 220 (2015) 441-447.
37. L. Wang, X. Lu, Y. Ye, L. Sun, Y. Song, *Electrochimica Acta* 114 (2013) 484-493.
38. H. Yin, Z. Cui, L. Wang, Q. Nie, *Sensors and Actuators B: Chemical* 222 (2016) 1018-1023.
39. L. Wang, Y. Zheng, X. Lu, Z. Li, L. Sun, Y. Song, *Sensors and Actuators B: Chemical* 195 (2014) 1-7.
40. Y. Song, C. Wei, J. He, X. Li, X. Lu, L. Wang, *Sensors and Actuators B: Chemical* 220 (2015) 1056-1063.
41. Y. Li, Y. Zhong, Y. Zhang, W. Weng, S. Li, *Sensors and Actuators B: Chemical* 206 (2015) 735-743.

© 2016 The Authors. Published by ESG (www.electrochemsci.org). This article is an open access article distributed under the terms and conditions of the Creative Commons Attribution license (<http://creativecommons.org/licenses/by/4.0/>).